Laboratori Nazionali di Frascati

LNF-88/38(P)
28 Giugno1988

B. D'Ettorre Piazzoli:

SURFACE AND UNDERGROUND EXPERIMENTS AT THE GRAN SASSO

Invited talk given at
Les Rencontres de Physique de la Vallée d'Aoste, la Thuile, Aosta Valley (Italy)
February 28 - March 5 1988

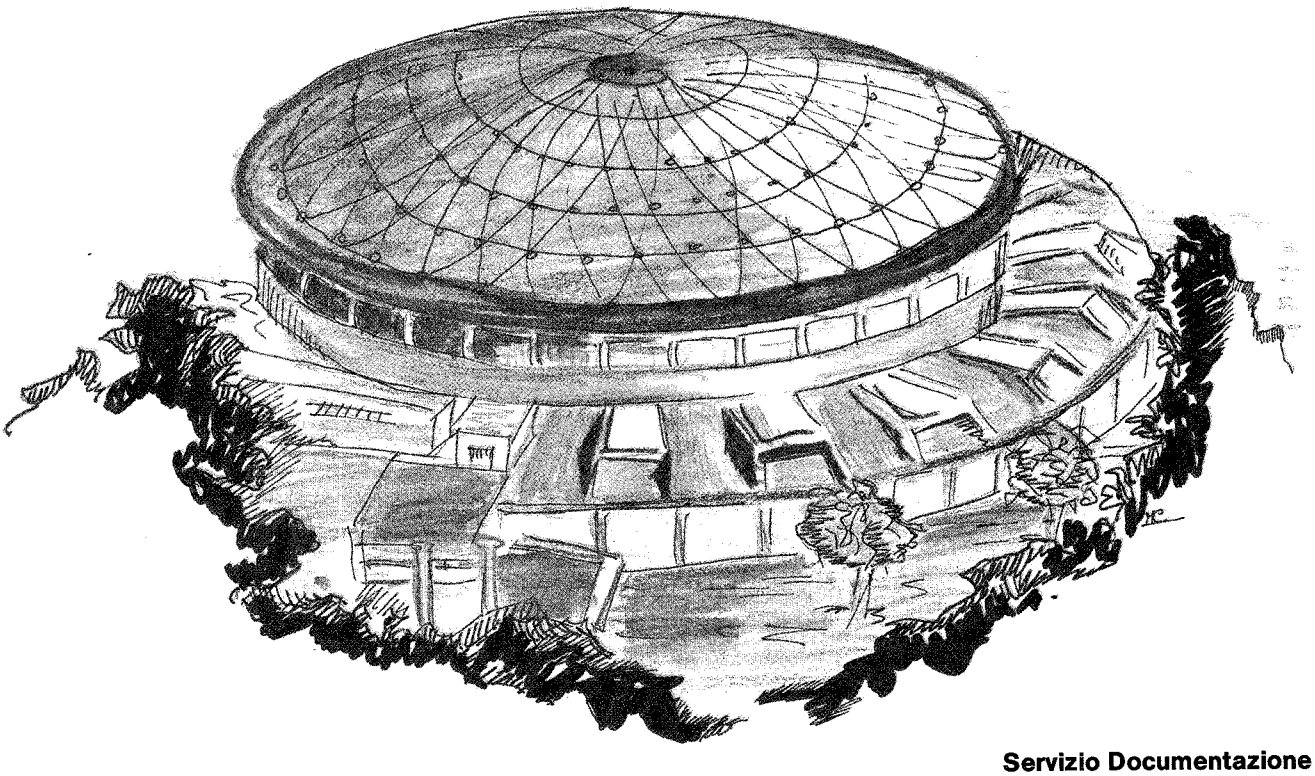

Servizio Documentazione
dei Laboratori Nazionali di Frascati
P.O. Box, 13 - 00044 Frascati (Italy)

ISTITUTO NAZIONALE DI FISICA NUCLEARE - ISTITUTO NAZIONALE DI FISICA NUCLEARE - ISTITUTO NAZIONALE DI FISICA NUCLEARE - ISTITUTO NAZIONALE DI

INFN - Laboratori Nazionali di Frascati
Servizio Documentazione

LNF-88/38(P)
28 Giugno 1988

SURFACE AND UNDERGROUND EXPERIMENTS AT THE GRAN SASSO

B. D'Ettorre Piazzoli

Istituto di Cosmogeofisica CNR - Corso Fiume, 4 Torino (Italy) and
INFN Laboratori Nazionali Frascati P.O. Box 13, 00044 Frascati (Italy)

ABSTRACT

Various aspects regarding the nature and origin of high energy (> 10^{14} eV) primary cosmic rays are still unsolved. The experimental information is obtained in an indirect way by means of measurements of the secondary particles produced in the atmospheric cascade. The sensitivity of the on-ground and underground detectors at the Gran Sasso Laboratory in performing these investigations is carefully analyzed.

INTRODUCTION

My purpose at this session devoted to the Astrophysics and Underground Physics is to examine the capability of the planned experiments at the Gran Sasso Laboratory in providing high sensitivity devices to study the nature and the origin of primary cosmic rays.

Cosmic rays are one of the principal constituents of our Galaxy. This is shown in Table I where the galactic power output of different types of radiation are compared. Their energy density is about 1 eV/cm^3, greater than the flux of light at the Earth due to all the stars (~0.6 eV/cm^3).

The knowledge of the properties of the primary cosmic rays, that is, chemical composition, energy spectrum and distribution of the arrival directions is of fundamental importance to model the cosmic-ray evolution: the production at the sources (galactic or extragalactic), the acceleration (statistical in the interstellar medium or direct at source) up to very high energies, and the propagation through the galactic volume. The solution of these problems will contribute to our knowledge of the properties of the Galaxy.

The current situation can be summarized broadly as follows. Up to about a few GeV per nucleon, the relative abundance of elements does not vary with energy and is very similar to the

Solar System (Sun and meteorites) abundances apart from an excess in cosmic rays of light elements Li, Be and B, and, to a minor extent, of the elements just lighter than iron, Fig. 1. These elements are not expected to be produced by fusion reactions in stars. It is assumed that a set of primary nuclei produced by sources are accelerated (at sources themselves or in the interstellar medium by diffusive shock acceleration) and diffuse inside the volume of the galactic disc (or halo). During the residence time, $10^6 \div 10^7$ years, they would have traversed about 6 g/cm^2 of matter thus producing through spallation the observed abundance of light elements. At higher energies the ratio of the secondary nuclei to the primary ones decreases with increasing energy. This implies an energy dependent path length presumably due to a higher probability for escape from the Galaxy or to a decreased residence time in the neighborhood of the sources. At energies around 10^{12} eV (= 1 TeV) primary species are essentially constituted of five groups - p, He, CNO, Si-Mg group, Fe group - whose relative weight is shown in Table II. Their energy spectrum follows a power law $dN/dE = E^{-\gamma}$ with spectral indices in the range $2.5 \div 2.8$, Fig. 2 and TABLE II. In spite of a large amount of experimental data and intense theoretical efforts, exact shape of these distributions at energies beyond 10^{12} eV is essentially unknown. Recently, emulsion chambers of large area flown on balloon[1] and transition radiation detectors flown on the Spacelab 2 mission of the Space Shuttle Challenger[2] provided precious direct measeurements of protons and nuclei up to 100 TeV/n and of heavier nuclei up to about 1 TeV/n.

There is an indication of a steady increase of the relative abundance of iron in cosmic rays up to ~ 10^{14} eV. According to theoretical models the differences in the power-law spectra should reflect either acceleration or propagation effects. Statistically significant direct measurements are expected to cover, in the next years, the energy gap 10^{12} - 10^{14} eV.

On the contrary, the chemical composition and the energy spectrum in the energy range $10^{14} \div 10^{16}$ eV corresponding to the so-called "knee" region where the spectrum of the primary cosmic rays appears to become steeper (see Fig. 3), can be investigated only in an indirect way from the analysis of the properties of the secondary particles produced in the atmospheric cascade. There is a great deal of astrophysical interest in this region because the steepening in the spectrum and the variation of the composition across the bend should reflect a feature of the source (the upper energy limit of the acceleration processes) and/or the failure of the galactic trapping.

However, the sensitivity of these experiments is rather poor and usually only general trends can be extracted. Moreover, the characteristics of the air shower phenomena in the atmosphere depend both on the chemical composition of the primary cosmic beam and on the hadronic interaction, so that the interpretation of these experiments depends on the model of high energy interactions used in the calculations. As a result, these studies have produced a very contradictory set of interpretations about the chemical composition at energies > 10^{14} eV.

Fortunately, recent data from accelerator experiments ($\sqrt{s}$ = 900 Gev) provide the characteristic features of the nucleon-nucleon interaction at energies close to 10^{15} eV. The kinematical regions covered by collider and cosmic ray experiments are only marginally overlapping because the high energy particles detected in these experiments come from the fragmentation region. In addition,

some uncertainties remain in describing the properties of particle production in nucleus-nucleus interaction, though all simulations confirm the reliability of the very simple superposition model. Nevertheless, the most important interaction features are rather well known, and only minimal extrapolations are needed to describe the particle production at energies as high as 10^{16} eV.

Thus a reasonable model of the development of the cascade in atmosphere up to these energies can be constructed and the measured features of the secondary particles used to obtain information about the primary beam. In this respect, studies of the frequency distribution of high energy (>1 TeV) muon bundles of different multiplicities appear to be the best way to disentangle the competing astrophysics and particle physics effects.

Muons detected far underground are the high-energy remnants of the first interactions of the primary cosmic ray beam. They do not decay (decay length $l_\mu = 6.2 \cdot E_\mu$ (GeV) Km to be compared to the production height 15 ÷ 20 Km), lose in the atmosphere only a very small fraction of their initial energy (ΔE (GeV) $\simeq 2.5 + 3.5 \cdot 10^{-3}$ E(GeV) for TeV muons) and arrive practically undisturbed at ground level together with the other air shower components. The rock above the underground laboratory acts as an energy analyzer absorbing all charged particles other than high energy muons.

Very large apparata in the Gran Sasso Laboratory offer an unique possibility of performing these studies. The threshold energy corresponding to a survival probability of 1% is 1.2 TeV in the vertical direction. (The effective energy as defined in Ref. (10) and corresponding to a survival probability of 30% is 1.7 TeV).Detectors should combine a large area with a good spatial resolution. The three major experiments LVD[5], MACRO[6], ICARUS[7] have different primary purposes but each of them satisfies these requirements (TABLE III) and appear well suitable to pursue this type of physics.

In addition, a large air shower array on top of the Gran Sasso mountain (EAS-TOP)[8] will operate in coincidence with the underground detectors to provide, by measuring the electron size N_e on the surface, an estimate of the primary energy. This array is located at an altitude of 2000 m a.s.l. (corresponding at a vertical atmosphere depth of 805 g/cm^2) and zenith angle $\theta = 27.5^o$ off the vertical from the underground laboratory for which the corresponding depth is about 3300 hg/cm^2 of standard rock, Fig. 4. This is a well implemented array planned to sample simultaneously electrons, muons and hadrons of $5 \cdot 10^{13} \div 10^{16}$ eV air showers. The basic parameters of the G. Sasso facility are given in TABLE IV.

The EAS-TOP array will be operated independently from the underground devices to search for ultrahigh energy (UHE, $E_\gamma > 10^{14}$ eV) gamma rays from the Northern identified or candidate sources. This is an other aspect of the problem of the origin of cosmic rays. In fact, were the detection of 10^{15} eV gamma rays confirmed, these sources should have accelerated charged hadrons (protons or ions) with energies at least up to ~10^{17} eV.

Cygnus X-3 has been the first source of high energy gamma rays to be detected. It is also the most powerful one, the total luminosity integrated over the whole energy range >10^{12} eV amounting to $L_\gamma \sim 4 \cdot 10^{36}$ ergs/s. Thus the total energy of the accelerated cosmic rays has to be of the order of

$5 \cdot 10^{38}$ ergs/s, a value comparable to the power in cosmic rays of the Galaxy. Thus a few sources like Cygnus X-3 shining over typical times of $10^4 \div 10^5$ years could account for all cosmic rays in the energy range $10^{14} \div 10^{17}$ eV. This is a pleasant scenario because the most conventional models of statistical acceleration are apparently incapable of attaining such energies[9] .On the other hand, cosmic rays of energies > 10^{17} eV could have an extragalatic origin.

However, there are many conflicting evidences in the experimental results up to the extent to suggest that the claimed signals are nothing but statistical fluctuations in the background air showers. EAS - TOP array has been designed to meet the necessity of improving the experimental sensitivity as a basic tool to clarify the present situation.

In the following sections the expected performances and the sensitivity of the on-ground and underground apparatus at the Gran Sasso Laboratory in these cosmic ray studies will be discussed.

1. - MUON BUNDLE STUDIES

1) Sensitivity to the composition

The rates R_n of events with exactly n muons in the detector can be calculated as follows

$$R_n = \Sigma_A \int \frac{dN(A)}{dE_o} P_n(E_o, A)\, dE_o$$

where dN/dE_o is the energy spectrum of nuclei of mass A and $P_n(E_o, A)$ is the probability of sampling n muons of a shower resulting from the interaction of a primary of energy E_o and mass A, integrated over the acceptance area of the apparatus. It depends only on the interaction properties of high energy hadrons and on the experimental conditions. As a result, the astrophysical and particle physics aspects enter in a well-defined and separate way into the calculation of the muon bundle rates.

Once the functions $P_n(E_o, A)$ have been calculated, trial compositions can be checked by comparing the experimental rates to the expected ones. The energy and type of the primaries is not known on an event by event basis. This is the main drawback of these studies, a common feature of all air shower experiments. Moreover the functions $P_n(E_o, A)$ extend very broadly over more than 3 energy decades preventing the investigation of the details of the energy spectrum.

The sensitivity of the muon groups to the composition arises from the different muon yields from nuclei of different mass and the same total energy. In fact, high energy heavy nuclei are more efficient than protons in producing TeV muons, Fig. 5. The asymptotic behaviour of the muon yield is

$$N\mu\,(Eo\,,\,A;>E\mu) = A\cdot\, f\left(\frac{E_\mu \cdot A}{E_o}\right) \rightarrow A^{1/4}\cdot\, f'\,(E_\mu/E_o) \qquad (1)$$

as established in numerous Monte Carlo studies[10]. This effect means that a composition richer in iron nuclei will exhibit more muon bundles of high multiplicity.

The calculation of $P_n\,(E_o,A)$ is a very complicated job which proceeds through the following steps[11]

a) Calculation of cascade showers in the atmosphere and propagation of high energy muons through the rock. In such a way the multiplicity distribution and the lateral spread at a given slant depth h of the muons produced by a primary of energy E_o and mass A can be obtained.

b) Parametrization of these results in terms of functions of h (depth), E_o, A and folding in the particular detector. This can be accomplished in an analytical way once the detector acceptance area and the pattern of the surrounding rock are known.

This procedure has been used in interpreting the NUSEX data, providing for the first time an absolute comparison between calculated and experimental multiple muon rates[12]. There is a clear indication in NUSEX data that the relative fraction of primary heavy nuclei does not increase significantly up to about 10^{16} eV even if the low statistics of high multiplicity events prevents one to draw any firm conclusion. But the rate of low multiplicity events ($m \leq 3$) which come from an energy region ($\leq 10^{14}$ eV) where primary cosmic rays spectra and hadronic interaction are rather well known is reproduced at a level of 20% or better. This is a good evidence that the whole procedure does work.

In view of the experimentation at Gran Sasso a new set of Monte Carlo cascade simulations has been performed with an improved interaction model taking into account the more recent results from $p\bar{p}$ collider concerning scaling violation in the central region, multiplicity, rapidity and transverse momentum distributions and their correlations, and including nuclear target effects as well as a fragmentation model to descibe the nucleus - air nucleus interaction[13].

The mean number of muons is again well descibed by the Elbert's formula (1) but the multiplicity distribution is no longer of Poisson type and is better described by a negative binomial distribution. Thus the probability of high multiplicity events is increased. On the other hand, this effect is mitigated in finite size detectors from being the events with higher than average multiplicity associated with broader lateral distributions. This follows from having included in the Monte Carlo an increase in the average transverse momentum with charge multiplicity.

According to simulation, the full containment radius at Gran Sasso is ~ 12 meters, Fig. 6, which makes the prediction of the expected rates to be not very sensitive to the muon lateral spread. At the same time these large area detectors will allow a verification of the p_T spectrum of the bulk of the particles produced in hadronic interactions (pions and kaons) as well as a measurement of muons with large transverse momentum coming from the decay of very heavy particles.

In order to study the sensitivity to the primary composition, the expected sensitivity of the LVD experiment at Gran Sasso - the experiment with the smaller acceptance area - has been checked

by considering its capability to distinguish between two compositions (Low energy composition, LEC, and the Maryland spectrum) and the capability to resolve an iron spectral index variation $\Delta\gamma=0.1$.

Low energy and Maryland compositions are two extreme compositions which bracket our expectations for the fraction of heavy nuclei in the primary beam[14]. The first is energy independent obtained by a straightforward extrapolation to high energies of the fluxes measured at ~100 GeV/nucleon. The differential spectral index is 2.71 for all nuclear species.

The Maryland spectrum has been derived by measurements on the time structure of hadrons near air shower cores. In this model the iron group has a spectral index of 2.39 making up about 65% of the primaries above $2\cdot10^{15}$ eV, while other groups have the same index of 2.68. In both composition models all components change their spectral index to 3 for $E_o>2\cdot10^{15}$eV.

In performing these calculations the LVD detector has been assumed to have a volume of 13 x 36 x 9 m^3. The minimum detector thickness that a muon must cross in order to be detected has been taken to be 4.5 m. LVD has a complicated geometry and this schematization is likely to produce a slight overestimation of the true rates. On the other hand, this volume corresponds to half the volume of MACRO so that at least the low multiplicity rates expected in this detector can be easily evaluated. (Accordingly, calculation of the $P_n(E_o, A)$ for MACRO should have required a CPU time twice as large).

The actual rock thickness along each direction has been derived from a detailed map of the mountain. The chemical composition has been taken into account in converting the Gran Sasso rock to standard rock (Z = 11, A = 22).

Fig. 7 shows the expected rates in one year of running time assuming the two trial compositions (upper dashed line for "Maryland", lower dashed line for LEC).Full lines have been obtained using a model of composition derived from the analysis of NUSEX data[12], with two values for the iron spectral index with a difference of 0.1. In Fig. 8 the contribution of each primary component to the rate of muon bundles of multiplicity 1, 6, 12 is plotted as a function of the energy E_o. These curves refer to the LEC model.

These findings lead us to the following conclusions:

1) Single muons are essentially due to interactions of primary protons and helium nuclei (≥90% according to the two models) at energies around 10^{13} eV. The absolute counting rate differs by about 15% due to the fact that the measured fluxes used for normalization are known with an accuracy on the order of 20%. Since the physics of the hadronic interaction is rather well understood at energies $<10^{14}$ eV and the proton and helium spectra are known to keep constant spectral index in this energy range, the single muon rate can be used to calibrate, with good precision, the proton and helium content at energies $5\ 10^{12} \div 10^{14}$ eV. This possibility has already been explored in the analysis of NUSEX data and should be considered further carefully.

2) Events with multiplicity ≥ 6 probe primary energies ≥ 10^{15} eV with high statistics. The expected rate of events with 12 muons in the detector (primary median energy ~ 10^{16} eV) for the two compositions differ by a factor 5 and are about 14σ away. One year exposure also provides a high

sensitivity to the slope of one single component; a 6σ difference for the two NUSEX compositions with $\Delta \gamma_{Fe} = 0.1$ is found at multiplicities corresponding to median energies beyond the cut-off ($m \geq 10$). This sensitivity is not achieved in a small size detector such as NUSEX due to the low statistics. This is shown in Fig. 9 where the expected rates are compared to the experimental ones collected in 5 years of data taking. (Note that the NUSEX composition has been folded to the results obtained with the upgraded Monte Carlo so that the agreement at the high multiplicities is not as good as in the previous analysis)

2) Surface-underground correlation

The main drawback in this type of experiment which uses the underground data alone is that the contribution to a given multiplicity comes from primaries whose energy spans at least two decades (see Fig. 8). This is an unpleasant situation which prevents a detailed investigation of the energy dependence of the cosmic ray composition.

The sensitivity to composition can be enhanced by tagging the underground muon events with the measurement of the shower size on the surface since the relation between size and primary energy differs by less than a factor of two for protons and iron, Fig. 10. As a consequence it is possible to measure muon multiplicities in fixed shower size windows corresponding to comparable total energies for all nuclear species.

The basic parameters for the operation of the surface-underground coincidence are shown in Table V and VI. Simulations with the present Monte Carlo show that the shower axis can be identified in the underground detector with an angular precision better than 0.3° (according to the multiplicity) while the core location is better than 2 meters for muon groups; single muons have a typical lateral dispersion of 4 m and an average scattering angle $\leq 0.5°$. [With a distance of 1170 m these numbers correspond to a core location at ground better than 10 m] EAS-TOP performances have been obtained with a separate Monte Carlo folding the air shower distributions to the array structure. Core location and angular resolution are better than 5 m and 1.5° respectively (the actual numbers depend on the shower size). Thus the geometry of the event can be defined with a good accuracy. The association of the surface and underground events is made easy by the low trigger rates (Table V).

Trigger rates and expected number of events refer to an underground detector of 500 m^2 area. In calculating the number of coincidences, only events with the shower axis falling on the underground detector area have been considered. Therefore this is a conservative estimate.

Not all the events recorded by EAS-TOP in the geometrical acceptance for combined operation [N(> E) in Table VI] will be actually accompanied by one or more muons in the underground detectors. The fraction of events having at least one muon in the underground detector is about 30% at 10^{14} eV and increases with energy being close to 100% at energies above the knee ($2 \cdot 10^{15}$ eV).

The expected rates of air shower detected by the surface-underground telescope for different energy ranges are shown in the last column of Table VI. About 25 events at energies $>10^{16}$ eV will be detected in one year of operation. In spite of the low statistics, a noticeable sensitivity can be achieved since most of these events are multiple muons which are produced with different efficiency by protons and heavy primaries at comparable total energies, (see Fig. 5). On the contrary for small showers ($E \sim 10^{14}$ eV) the main contribution is due to single muons primarily from cosmic ray protons. Since the proton spectrum and the interaction features in the 100 TeV region are both rather well known these events will provide an useful calibration point for the joint operation of the surface and underground detectors.

In order to quantify the previous considerations, the expected muon multiplicity distributions for some wide intervals of the electron size N_e are shown in Fig. 11. Contributions from protons, CNO and Fe nuclei have been singled out. The expected distributions according to LEC and Maryland compositions are shown for selected showers in the size window $10^6 < N_e < 3 \cdot 10^6$ corresponding to $3 \cdot 10^{15} < E < 2 \cdot 10^{16}$ eV, i.e. above the knee for any primary mass. The error bar indicates the sensitivity that can be obtained in two years of operation.

3) Sensitivity to the interaction model

Multiple muon rates are primarily sensitive to charged meson multiplicity distribution and to the particle generation in the fragmentation region.

The muon multiplicity distribution is well described by a negative binomial distribution whose parameters depends on E_o, A, h. This is one of the main differences (the other one concerns the lateral distribution) with respect to the previous Monte Carlo simulations producing muon distributions rather well described as a Poissonian. In fact, in these simulations the multiplicity distribution of the charged parent mesons is not taken into account and the energy of each particle is sampled according to the inclusive distribution until the whole energy available for secondary production has been utilized. This procedure generates poissonian-like distributions. For a given average value N_μ, the use of a Poisson distribution instead of a negative binomial one decrease the probability $P_n(E_o, A)$ for high multiplicities and, finally, the rate R_n. This effect has been checked for NUSEX detector (differences up to 70% have been found for the highest multiplicities n = 5,6).

For 2 TeV muons and primary energies near 10^{14} eV the contribution comes from $x_F>0.03$ corresponding to $\eta > 3.5$. For an increasing primary energy the contribution of the central region grows and above 10^{15} eV a large fraction of the underground muons come from mesons produced with lower x_F. However, the fragmentation region continues to provide the bulk of the events. Thus a broad kinematical region of interest for underground measurements is not covered by accelerator data even if there is an indication of scaling, valid up to 10 - 20%[15].

On the contrary, due to the large area of the detectors, the detail of the transverse momentum distribution for $p_T < (E_\pi \cdot l/h) \sim 2$GeV/c [$E_\pi$ = mean energy of the parent pion ~ 4 TeV, h =

generation height ~ 19 Km, l = typical linear dimension of the detector ~ 10 m] are not important, at least for energies below the knee.In fact at collider energies more than 99% hadrons are produced with low - p_T (< 2 GeV/c) [but in the energy range $\sqrt{s}$ = 1 ÷ 15 TeV (E=5·10^{14}÷10^{17}eV) a sizeable fraction of hadrons could be produced at higher momenta].

In the present cascade simulation the final state of the interaction is reproduced by means of a "cluster" Monte Carlo, rather close to the Monte Carlo generator developed by the UA5 collaboration at CERN, but modified to include target effects[16]. Thus the extrapolation to $\sqrt{s}$ = 15 TeV is made using data up to collider energies ($\sqrt{s}$ = 900 GeV) in the context of inelastic 'ln s' physics. Scaling validity in the fragmentation region is predicted.

Though it is very hard to estimate the region of validity of this phenomenological treatment, some simulations performed with modified parameters show that the uncertainties on the estimated rates should not exceed 30% unless new physics changes radically the properties of the nucleus-nucleus interaction, as for instance suggested by the unusual cosmic ray events Centauros, Chirons etc. seen in the air-family data or according to the predictions of a possible phase transition to quark-gluon matter. In the latter case, the muon yields of heavy primary nuclei could increase due to the abundant production of charm and higher flavor particles. Apart from this exception, calculations of muon rates seem reasonably reliable and the experimental data itself could be used to set evidence for possible "new" effects.

2. - UHE GAMMA RAY ASTRONOMY WITH THE EAS-TOP ARRAY

High energy γ-ray astronomy was born on September 1972 when an excess (~17%) of TeV γ-rays from the direction of Cygnus X-3 was detected by the Cerenkov Telescope of the Crimean Astrophysical Observatory, about a week after the maximum of a large radio-flare (Fig. 12).
The detection of the atmospheric Cerenkov light emitted by fast electrons (E_e > 21 MeV at sea level) in γ-ray initiated air showers was suggested as early as 1961 by Zatsepin and Chudakov[17] following the Cocconi proposal[18] of using air shower arrays for the search of discrete γ-ray sources. Both these techniques are now widely exploited. The energy range 10^{11}÷10^{14} eV where Cerenkov γ-ray telescope are used is called very-high energy (VHE) while the range above 10^{14} eV where air shower electrons are detected is referred to as ultra-high energy (UHE).

Showers in excess of 10^{13} eV reach the ground with an electron size which depends on the altitude. The number of electrons and their lateral distribution at the G. Sasso altitude in γ-ray initiated air showers are shown in Fig. 13. More than 10^4 electrons at ground level are produced by primary photons of 10^{14} eV. Within about 100 m from the shower axis these electrons are contained in a thin disc (a few nanoseconds) perpendicular to the direction of the initial γ-ray or cosmic-ray. By fast timing technique the orientation of the disc is reconstructed, hence the direction of the primary particle. For ~ 1° resolution, a nanosecond accuracy is required.

Over a nine year period (1972-1980) the Crimean group accumulated sufficient data to identify the 4.8 hour periodicity obtained from x-ray observations. However the light-curve is not an aymmetric sine wave as in the x-ray band, the emission being concentrated in narrow phase intervals ("beaming effect") at phases 0.15 ÷ 0.2 and 0.6 ÷ 0.8.($\varnothing$ = 0 corresponds to the x-ray eclipse.). The relative amplitude of the two peaks was not stable with time. The flux was found to be highly variable with a mean intensity corresponding to a γ-ray luminosity $L\gamma$ ($\geq$ 2 TeV) ~ $5 \cdot 10^{36}$ ergs/s very close to the total x-ray luminosity. Occasionally sporadic radiation has been detected unrelated to the 4.8 hour phases.

Later, several other groups[19] reported the detection of Cygnus X-3 using ground-based atmospheric Cerenkov techniques. Taken as a whole, these data are in broad agreement with the Crimean results and confirm the high time variability of the source both in amplitude and phase of emission.

Cygnus X-3 is the most extensively studied source. This is not only due to historical reasons but also to its peculiarity. It is one of the most powerful sources in the Galaxy (L_x~ 10^{38} ergs/s, see Table VII) exhibiting modulated emission at radio, infrared, x-ray and possibly γ-ray wavelengths. Unfortunately it lies so close to the galactic plane that the optical counterpart has never been observed.

At all wavelengths, the main characteristic is its variability. The radio emission displays periods of enhanced activity and the occurrence of giant radio flares with flux increasing by more than 10^3 times the queiescent level and reaching luminosity of 10^{35} ergs/s. In the infrared range sporadic flares lasting from minutes to hours are observed superimposed over the periodic modulation . Even in x-ray it exhibits variability from cycle to cycle, transient sporadic fluctuations and long term variations eventually associated to other periodicities.Thus Cygnus X-3 is anything but a steady source: it is a system in violent activity where different mechanisms are operating to produce the radiation observed in different energy ranges. The variability at the highest energies is likely to be associated with the difficulties to fulfil the geometrical and physical constraints required to achieve the particle acceleration and subsequent γ–ray production.

Three other X-ray binary pulsars have been observed in the TeV region, Hercules X-1, 4UO115 + 63, Vela X-1; (the binary nature of Cygnus X-3 is still unproved but it is commonly accepted that the 4.8 hour modulation is produced by orbital motion around a companion star). The list of TeV γ-ray sources also includes radio pulsars, (Crab Pulsar, Vela Pulsar, PSR 1953+29, PSR 1082 - 23, PSR 1937 + 21), supernova remnants (Crab Nebula) and radio Galaxies (Cen A). It seems clear that many radio and x-ray pulsars are powerful VHE γ-ray sources.

Models proposed to explain the high energy γ-ray production differ greatly in what concerns the way of achieving large potential differences, the nature of the accelerated particles, the source geometry and the radiation mechanism. Although the γ-ray production mechanisms might be quite different for these classes of objects - and eventually among the binary sources themselves - the proposed models take into consideration essentially either bremsstrahlung and/or curvature radiation of $\leq 10^{14}$ eV electrons or the interaction of an hadronic beam with some target material producing

π^o's and hence gamma-rays. The latter mechanism seems mandatory at the highest energies since the increasing energy-loss rate by synchrotron emission and inverse Compton emission should prevent the electrons to reach energies above 10^{15} eV.

In this picture, UHE γ-ray ($E_\gamma > 10^{14}$ eV) testify the existence of discrete sources where energetic cosmic rays up to 10^{17} eV are generated. They are the only objects known to accelerate particles to such energies.

First evidence of UHE γ-ray from Cygnus X-3 came from the reanalysis of the observations made in the 10^{16} eV energy band at Kiel and at Haverah Park, Fig. 14. These observations have been confirmed by other experiments but with weaker evidence.Evidence has been reported also for emission from other sources as summarized in Table VIII.

In the UHE range Cygnus X-3 is the only source observed by more than one experiment. Even in this energy range there is strong evidence for variability. Phase of the emission moved during the years from $\varnothing$ ~0.1 ÷ 0.2 to $\varnothing$ ~0.6 ÷ 0.7 (Fig. 15). Data taken in different years exhibit considerable scatter in the measured fluxes. In addition to the long-term observations, episodes of enhanced emission have been reported, sometimes correlated to giant radio flares. Finally there is some evidence that the flux is steadily decreasing on a time scale of a few years.

This complicated phenomenology has to be faced with implemented arrays. The main problems concern essentially the low statistics and the nature of the primary radiation.

Apart from a few exceptions the claimed detections are of rather low statistical significance, < 4σ after phase analysis[19]. This means that the excess counting rate from the source direction is not sufficient to establish the existence of the source. Only in the Kiel experiment a D.C. excess of 4.4σ has been measured from the direction of Cygnus X-3. (At the recent Moscow Conference the detection of a 3.8σ D.C. excess of > 10^{15} eV γ -rays from the direction of Cignus X-1 has been reported[20a]). All experiments use phase analysis in order to identify a positive excess from a candidate source. This is a very disturbing aspect in view of the time variability of the emission phase, of the presence of burst-type activity and since many effects might cause a non uniform background distribution. This can result in a flux intensity dependent upon the source ephemeris adopted or in a misidentification of the signal. On the other hand the phase analysis provides geometrical information about the relative orientation of the source of the beam and the target. Again, this study requires a sample of events with improved signal to noise ratio.

To overcome these problems the sensitivity of the air showers arrays needs to be improved. The sensitivity depends on the ratio $A^{1/2}/\delta\theta$ (A = effective area, $\delta\theta$ = angular resolution). Air shower arrays not dedicated to γ-ray astronomy operate in this energy range with $A \leq 10^4$ m^2 and $\delta\theta > 1^o$. This is not enough to achieve the required sensitivity. On the contrary, an array having at PeV energies an effective area as large as 10^5 m^2 and pointing to Cygnus X-3 within 1.5^o ($\delta\,\theta < 1^o$) could detect in one year of data taking about 230 events against a background of 4400 events, that is a 3.5σ effect solely from the counting rate analysis.

A high sensitivity array with good energy resolution < 50% could explore the shape of the energy spectrum of Cygnus X-3 in the important range 10^{15} - 10^{16} eV where an absorption dip is

expected due to the $\gamma\gamma \rightarrow e^+e^-$ pair production process on the microwave photons of the 2.7° K black body background, Fig. 16. This should be the more striking evidence that the primaries are gamma rays, which is questioned, as discussed below. Moreover a statistically significant sample of events at energies > 10^{16} eV could be detected (~ 20 ev/year assuming an E^{-1} behavior) to check the existence of the energy cut-off exhibited by the Haverah Park data (based on 9 events observed in 4 years of data taking) but not present in the Kiel data.

A puzzling problem concerns the nature of the primary particles detected in these experiments. Primaries are not positively identified as gamma rays, this conclusion being reached by eliminating neutrons and neutrinos, the only known neutral particles, and invoking "continuity" from observations at lower energies.

Two distinguishing features have been exploited in order to enrich the sample in "γ-ray showers" with respect to the "cosmic ray showers": (i) the age parameter, (ii) the muon density. The energy degradation is quite faster in γ-ray initiated showers ($\lambda_\gamma \sim (9/7) \cdot \lambda_{r.l.} \sim 50$ g/cm^2) than in cosmic ray initiated showers which are continuously fed by nuclear interactions. Thus "γ - ray showers" are expected to have, on average, larger age parameter s than cosmic ray showers. In the Kiel (Cygnus X-3) and Adelaide (Vela X-1) experiments the source signal is found only in the high s showers, but no s-cut has been used in analyzing Haverah Park and Akeno data. To further complicate the situation, some recent Monte Carlo simulations found that the ages for high energy "γ-ray showers" are smaller than for "cosmic ray showers".

A few muons are expected in γ initiated showers, arising from the decay of $\pi^\pm$ produced in photomeson production processes. All calculations indicate a muon content ≈ 0.1 of that of a cosmic ray initiated shower. This expectation is based on the fact that typical photonuclear cross sections are 0.5% of the proton nuclear cross section.Only a few experiments have muon detectors. Some of them found evidence for emission only when muon-poor showers are selected [BASJE (Vela X-1, Cen X-3) and Akeno (Cygnus X-3)]But other experiments [Kiel (Cygnus X-3), underground flash lamps; M.S.U. (Cygnus X-1), underground spark chambers; Los Alamos (episodes of emission from Cygnus X-3 and from Hercules X-1), shielded MWPC] found a muon content very close to that of cosmic ray showers[20a]. It is not easy to asses the statistical significance of these results since in these experiments the muon detectors are of limited area (< 100 m^2) and the muon density in air shower is only a few percent of the electron density and is known to fluctuate significantly.

In conclusion, even if on the whole there is a measure of consistency between the data at TeV energies, the reported observations in the UHE range are rather poor and display some conflicting results. Time variability and unusual results require more sensitive apparata providing accurate measurements of all shower components. Redundancy is welcome. Arrays located at similar longitudes could compare data taken over identical times. Arrays located at different longitudes are expected to provide a continuous monitoring of the sources (in fact, due to the increasing atmospheric depth with zenith angle the observations of the sources is limited to only a few hours each day depending on the altitude and latitude of the site and on the declination of the source).

EAS - TOP array at Gran Sasso will operate with high sensitivity in the field of the UHE γ - ray astronomy in order to face the quoted problems. It is rather close in longitude to GREX array at Haverah Park and together with the planned or operating U.S.A. and Asian arrays, it will allow a monitoring of Cygnus X-3 over at least 80% of time[22].

The following parameters will be measured:

a) electron densities at different points in order to obtain the lateral distribution of particles and therefore the shower "age" s and the shower size N_e ($\Delta E/E \leq 40\%$);

b) arrival times at the different points (instrumental resolution $\delta t \leq 1.5$ ns) in order to get the arrival directions by means of the time-of-flight technique ($\delta\theta \leq 1^o$);

c) the muon and hadron content (and hadron spectrum at high energies).

The detection of the electromagnetic component is accomplished by means of 28 modules (10 m^2 scintillators each) separated in the central part of 15 ÷ 25 m and in the external part of 50 ÷ 70 m, in order to operate with good efficiency in the whole energy range $5 \cdot 10^{13} \div 10^{16}$ eV. The covered area is 10^5 m^2. Fast photomultipliers coupled to leading fast electronics exploiting double threshold technique guarantee the required angular resolution (by time of flight). The main performances as obtained by Monte Carlo simulations are reported in Table IX. Half of the scintillation counters are already working and preliminary analysis confirm the expected accuracy in timing[21a].

Two muon-hadron detectors, 140 m^2 each, made of 9 layers of streamer and proportional tubes separated by iron absorbers will track ($\delta\theta \leq 1^o$) the low-energy muons ($E\mu > 2$ GeV) and measure the hadron spectrum at high energies ($E_H > .5$ TeV, $\delta E_H/E_H < 30\%$)[21b].

In Fig. 17 the minimum detectable flux from Cygnus X-3 ($\varnothing_m$) at 3 standard deviation level in one year of operation before phase anlaysis is compared to the experimental intensity. It results $\varnothing_m \sim 1/2\ \varnothing_{cyg}$ at energies $> 5 \cdot 10^{14}$ eV. More than 200 ev/year are expected at energies $> 2 \cdot 10^{15}$ eV. The same figure for Kiel and Haverah Park arrays is 16 ev/4 years and 60 ev/4 years respectively. In doing this calculation an observation time of about 6 hours per day has been taken in account. The observation time per day is shown in Fig. 18 as a function of the declination of the source. The array has been assumed to be sensitive to air showers from within 35° of the zenith. This corresponds, at the altitude of the site, to an atmospheric depth of ~ 985 g/cm^2. For other candidate sources in the Northern Hemisphere (Her X-1, 4U0115 + 63, CRAB, GEMINGA) $\varnothing_m$ can be easily obtained scaling the curve of Fig.17 by the factor $(t_{oBS}/6)^{1/2}$ where t_{oBS} is the observation time per day given in Fig.18. Thus the minimun detectable flux from Hercules X-1 is only 20% higher than that from Cygnus X-3.

The minimum detectable flux for a transient burst lasting one day, using the same criteria, is about 20 times larger. Hercules X-1 has been observed as a source of PeV γ rays during a 40 minute outburst with a transient flux of $3.3 \cdot 10^{-12}$ cm^{-2} s^{-1} (Fly's Eye). Such an event should give 8 events against a background of 0(1) events with $E > 10^{15}$ eV. This is more than the 1.8 σ excess reported by Fly's Eye, but the statistical significance is rather marginal and a positive detection should require, in this case, a search for modulation.

If data will confirm that the muon content of γ-ray showers is much less than that of cosmic ray showers a rejection of more than 90% of hadron initiated showers could be achieved. That means a further reduction of a factor three of $\varnothing_m$. In this respect the study of the muon content in showers with core distance from the muon detector $R < 60$ m will be of primary importance. For instance, hadron initiated showers of $E = 5 \cdot 10^{14}$ eV with core at 50 m are expected to give on average 30 muons on the detector while the mean muon number from a gamma primary is expected to be as low as 2. The efficiency of the muon veto depends on the fluctuations of the muon number in the shower. These are known to be broader than a simple Poissonian. The first year of operation should be sufficient to understand this crucial point in order to optimize the area (> 500 m^2) and the distribution of other muon-tracking detectors over the whole array area. Were the muon content of excess showers associated to Cygnus X-3 larger than the expectation, an exotic effect should exist and the extension of the array will allow systematic studies on the nature of the primary particles and their interaction by correlating many characteristics of such showers (size, age, low energy muon and hadron content).

CONCLUSIONS

I apologize for some omissions due to lack of time (at the oral session) and space. They concern the capability of the underground detectors to study the muon signal from the direction of the Northern sources (NUSEX[27] and SOUDAN[28] detection of a muon excess from the direction of Cygnus X-3; the sensitivity of the Gran Sasso arrays is about a factor 10 larger) and the capability of detecting the neutrino-induced muon events from Southern massive systems like LMC X-4. A few events per year in a 1000 m^2 array can be expected from this source in an optimistic scenario, a rather marginal but very important detection (if any). These are other aspects of the search for cosmic sources. The primary composition will be studied by EAS-TOP array also in its autonomous operation. We expect the large area, with consequent increase in statistical power, the good angular accuracy and the sampling of all components to allow us to make significant contributions to the studies of the cosmic ray anisotropies and shower phenomenology.

Two arrays are presently under construction at the Gran Sasso Laboratory, the EAS-TOP array and the MACRO detector. The installation of both devices will be completed at the end of 1989. The installation of the LVD detector is scheduled for the end of this year. Starting from 1990 a facility including a large area surface array over large acceptance underground detectors will be operating at the Gran Sasso with high sensitivity in the field of the origin and nature of the primary cosmic rays.

ACKNOWLEDGEMENTS

I woulk like to acknowledge the work done by my colleagues H. Bilokon, C. Forti, T.K. Gaisser and L. Satta in developing the Monte Carlo simulation. I thank G. Navarra for many useful discussions concerning the EAS-TOP array. I am very grateful to Mrs. L. Invidia and C. Farina for their invaluable help in preparing this paper.

Finally it is a pleasure to thank G. Bellettini and M. Greco for their hospitality and their support at La Thuile.

REFERENCES

(1) T.H. Burnett et al., Proc. 20th ICRC (Moscow), 1, 375 (1987).

(2) J.M. Grunsfeld, J. L'Heureux, P. Mayer, D. Muller, S.P. Swordy, Ap.J., 327, L31 (1988).

(3) J.A. Simpson, Ann. Rev. Nucl. Part. Sci., 33, 323 (1983).

(4) J. Linsley, Proc. 18th ICRC (Bangalore), 12, 135 (1983).

(5) C. De Marzo et al. (MACRO collaboration) Nuovo Cimento 9C, 281 (1986).

(6) C. Alberini et al. (LVD collaboration) Nuovo Cimento 9C, 237 (1986).

(7) L. Bassi et al. (ICARUS collaboration), INFN/AE-85/7 Frascati (1985).

(8) M. Aglietta et al. Nuovo Cimento 9C, 262 (1986).

(9) A.M. Hillas, Proc. 19th Rencontre de Moriond, High Energy Astrophysics (ed. J. Tran Thah Van), p. 11, (1984).

(10) T.K. Gaisser and T. Stanev, Nucl. Instr. and Meth., A235, 183 (1985).

(11) G. Bologna, A. Castellina, B. D'Ettorre Piazzoli, G. Mannocchi, P. Picchi and S. Vernetto, Nucl. Instr. and Meth., A234, 581 (1985).

(12) G. Bologna et al., Nuovo Cimento 8C, 93 (1985).

(13) H. Bilokon, B. D'Ettorre Piazzoli, C. Forti, T. R. Gaisser and L. Satta "High Energy Air Showers and Cascade Study", presented to the 20th ICRC, Moscow 1987. A detailed paper is in preparation.

(14) See Ref. [10].

(15) G. J. Alner et al. CERN-EP/86-126.

(16) See Ref. [13]. A description of the Monte Carlo simulation is given also in C. Forti, "Studio della cascata adronica ed elettromagnetica indotta da raggi cosmici di altissima energia. Applicazione a rivelatori in quota e sotterranei". (Thesis, Rome 1988).

(17) G.T. Zatsepin and A.E. Chudakov, Sov. Phys. JEPT, 41, 655 (1961).

(18) G. Cocconi, Proc. Moscow Conf. on Cosmic Rays 2, 309, (1959).

(19) For a summary see A.A. Watson in: Proc. 19th ICRC (La Jolla) vol. 9, 111, 1985 and T.C. Weeks, "Very High Energy Gamma-Ray Astronomy", Phys. Reports 160 (1988).

(20a) R.J. Protheroe, "Gamma Ray Astronomy at Energies Above 0.3 TeV", Rapporteur paper to be published in the Proc. 20th ICRC (Moscow 1987).

(20b) R.J. Protheroe, Proc. Astron. Soc. Australia, 6, 280 (1986).

(21a) M. Aglietta et al. Proc. 20th ICRC (Moscow), 2, 454 (1987).

(21b) M. Aglietta et al. Proc. 3rd Cosmic-Physics National Conference St. Vincent 1986, 7, 21 (1986).

(22) The Haverah Park GREX array has been in operation since 1985. It includes a small muon telescope (~40 m^2) See G. Brooke et al. in: Proc. Workshop on Techniques in U.H.E. Gamma-Ray Astronomy (La Jolla 1985). Los Alamos Cygnus array[23] and the University of Utah Extensive Air Shower Array[24] (enclosing the Fly's Eye II air scintillation detector) are operating in U.S.A.. Planned experiments include the GRAND array[25] (Notre Dame) and the CASA array[26] (Chicago). A new array called ORION & PEGASUS is planned by a Japan-China collaboration to be located at an elevation of about 4300 m in Tibet. (See Ref. 20a).

(23) B.L. Dingus et al., Phys. Rev. Lett., 60, 1785 (1988).

(24) R.M. Baltrusaitis et al., Proc. 20th ICRC (Moscow) 2, 435, (1987).

(25) J. Poirier, E. Funk, J. Lo Secco, S. Micocki, T. Reltig, ibid., 2, 438 (1987).

(26) M.R. Campbell et al., "A Proposal for a Large Surface Array at Fly's Eye II".

(27) G. Battistoni et al., Phys. Lett., 155B, 465 (1985). For an updated analysis see B. D'Ettorre Piazzoli, "Cygnus X-3 muon signal in the NUSEX Experiment", Proc. Vulcano Workshop 1986, 8, 277 (1986).

(28) M.L. Marshak et al., Phys. Rev. Lett. 54, 2079, (1985) and 55, 1965 (1985).

TABLE I - Power output of the Galaxy (ergs/sec).

Radio and microwaves	10^{39}
Optical radiation	10^{44}
X-Rays	$2 \cdot 10^{39}$
Cosmic Rays	10^{40}÷10^{41}

TABLE II - Composition at 1 TeV (kinetic energy per nucleus).

Group	Z	Elements	Relative Fraction	Spectral index γ
P	1	protons	42 ± 6	2.7 ÷ 2.8
α	2	Helium nuclei	20 ± 3	2.7 ÷ 2.8
CNO	3-5	Light nuclei	0.6 ± 0.2	2.6 ÷ 2.75
	6-8	Medium nuclei	14 ± 2	
Si-Mg	10-14	Heavy nuclei	10 ± 1	2.5 ÷ 2.7
	16-24	Very heavy nuclei	4 ± 1	
Fe	26-28	Iron group nuclei	10 ± 2	2.4 ÷ 2.7

TABLE III - Main characteristics of the deep underground detectors (h > 3000 hg/cm^2) for cosmic ray studies.

	PRESENT DETECTORS				GRAN SASSO DETECTORS		
	Nusex	Frejus	Kolar	Homestake (LASD)	MACRO	LVD	ICARUS
Vertical depth (hg/cm^2)	5000	4600	6050	4200	3600	3600	3600
Effective Area (m^2)	15	100	60	160	850	500	700
Spatial Resol.(cm)	1	.5	10	15	3	1	.2
Angular Resol.(°)	.5	.2	2	3	.2	.5	.1

TABLE IV - Basic parameters of the Gran Sasso Facility.

	UNDERGROUND DETECTORS	SURFACE DETECTOR (EAS-TOP)
LATITUDE	42° 27' 09" N	
LONGITUDE	13° 34' 28" E	13° 34' 13" E
ALTITUDE (m a. s. l.)	963	2000
ATMOSPHERIC DEPTH (g/cm^2)	780	805
TOP/UNDERGROUND PARAMETERS		
ZENITH ANGLE (°)		27.5°
ATMOSPHERIC DEPTH (g/cm^2)		908
SLANT DEPTH (hg/cm^2)		3360

TABLE V - Trigger rates and expected resolutions of the EAS parameters.

	SURFACE	UNDERGROUND (500 m^2)
TRIGGER RATES (Hz)	30	.5
EXPECTED RESOLUTION		
Core location at ground (m)	< 5	< 10
Direction (°)	< 1.5	< . 5

TABLE VI - Surface (EAS-TOP) underground (500 m^2) coincidence.

ENERGY (eV)	N (> E) (ev/yr)	N (ΔE) (ev/yr)
10^{14}	$1.1 \cdot 10^4$	
		4000
$5 \cdot 10^{14}$	$2.5 \cdot 10^3$	
		1850
$3 \cdot 10^{15}$	$2.1 \cdot 10^2$	
		180
10^{16}	25	

N (>E) = Integral number of showers recorded by EAS-TOP in the geometrical acceptance for the surface-underground coincidence.

N (ΔE) = Number of showers in the energy range ΔE with at least one muon in the underground detector.

TABLE VII - x-ray luminosity of binary sources.

GALACTIC	L_x (ergs/sec)
CYGNUS X-3	~ 10^{38}
HERCULES X-1	~ $7 \cdot 10^{36}$
4U0115 + 63	~ 10^{35}
VELA X-1	~ $6 \cdot 10^{36}$
EXTRAGALACTIC	
LMC X-4	~ $4 \cdot 10^{38}$
CEN X-3	~ $8 \cdot 10^{37}$

Apart from 4U0115 + 63 all these binary systems have been identified as UHE γ-ray sources [Taken from Ref. 20b].

TABLE VIII - PeV Gamma-Ray Source Catalog [1 PeV = 10^{15} eV].

	SOURCE	Periodicity	Integral Flux ($cm^{-2}\,s^{-1}$)	Luminosity (ergs/sec)+
	CYGNUS X-3	4.8 h (orbital)	$2 \cdot 10^{-14}$ (> 1 PeV)	10^{36}
	HERCULES X-1	1.24 s(pulsar)	$3 \cdot 10^{-12}$ (> 1 PeV)*	$2 \cdot 10^{37}$ *
(s)	VELA X-1	8.97 d(orbital)	$9 \cdot 10^{-15}$ (> 3 PeV)	$2 \cdot 10^{34}$
(s)	LMC X-4	1.41 d (orbital)	$5 \cdot 10^{-15}$ (> 10PeV)	10^{38}
	CYGNUS X-1	5.6 d (orbital)	$5.4 \cdot 10^{-13}$ (> 1 PeV)	10^{36}
	CANDIDATE SOURCES (Very poor statistical evidence).			
(s)	CEN X-3 (binary x-ray)	2.1 d		
	CRAB NEBULA (Supernova Remnant)	variable	$1 \cdot 10^{-13}$ (> 1 PeV)	$2 \cdot 10^{35}$
(s)	CENTAURUS A (Radio Galaxy)	steady		

(*) 40 minute outburst reported by Fly's Eye.
(s) Not visible from the Northern Hemisphere.
(+) The luminosities quoted assume 4π geometry. For some beam geometries this may be a significant overestimate.

TABLE IX - EAS-TOP performances.

ENERGY (eV)	$A_{eff.}$ (m^2)	$\delta\theta$ (degrees)
$5 \cdot 10^{13}$	10^4	1.6
10^{14}	$2 \cdot 10^4$	1.3
10^{15}	10^5	< 1
10^{16}	10^5	< 1

RESOLUTIONS INSIDE THE WHOLE ENCLOSED AREA FOR PURE E.M. CASCADES AT $E_\gamma = 10^{15}$ eV.

SIZE	N_e	< 15%
AGE	S	≤ 10%
CORE LOCATION (m)		≤ 5

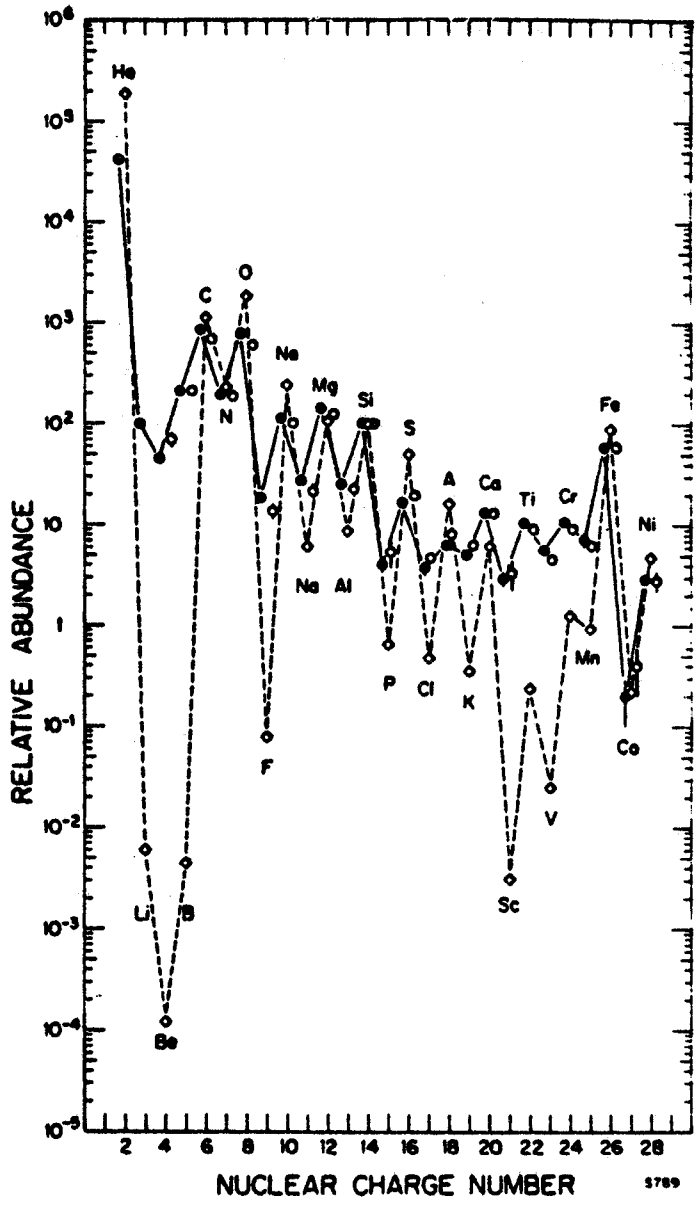

FIG. 1 - Comparison of the elemental abundances of cosmic rays and Solar System abundances. The two have been normalised at Silicon (Si = 100).
Solid circles: cosmic rays, Kinetic energy < 300 MeV/n;
Open circles: cosmic rays, Kinetic energy 1000 ÷ 2000 MeV/n;
Diamonds : Solar system.
[Taken from Ref. (3)].

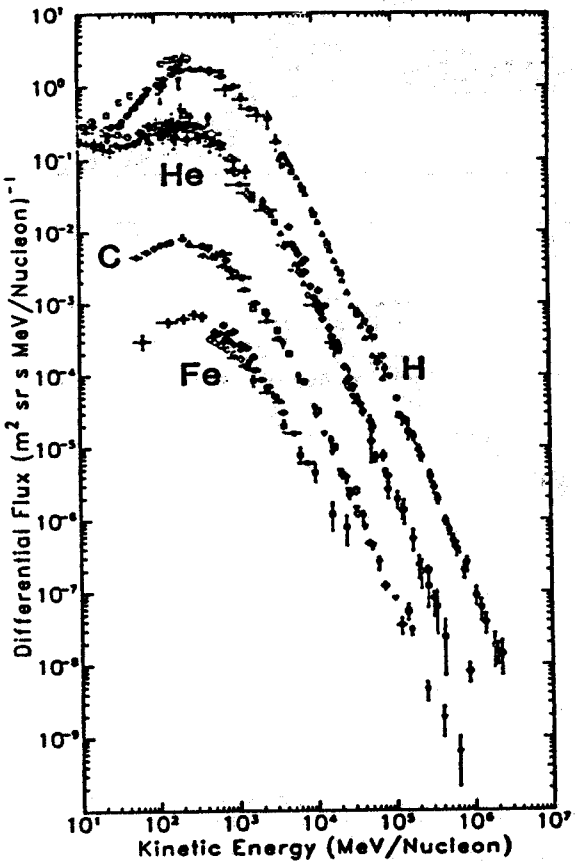

FIG. 2 - Differential energy spectra of cosmic rays for the elements hydrogen, helium, carbon an iron measured near earth. [Taken from Ref. (3)].

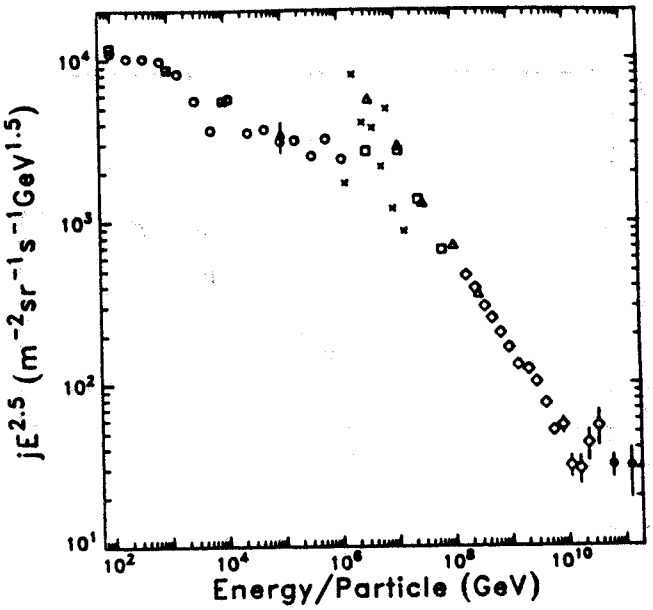

FIG. 3 - The all-particle differential energy spectrum at Earth as compiled by Linsley, Ref.(4).

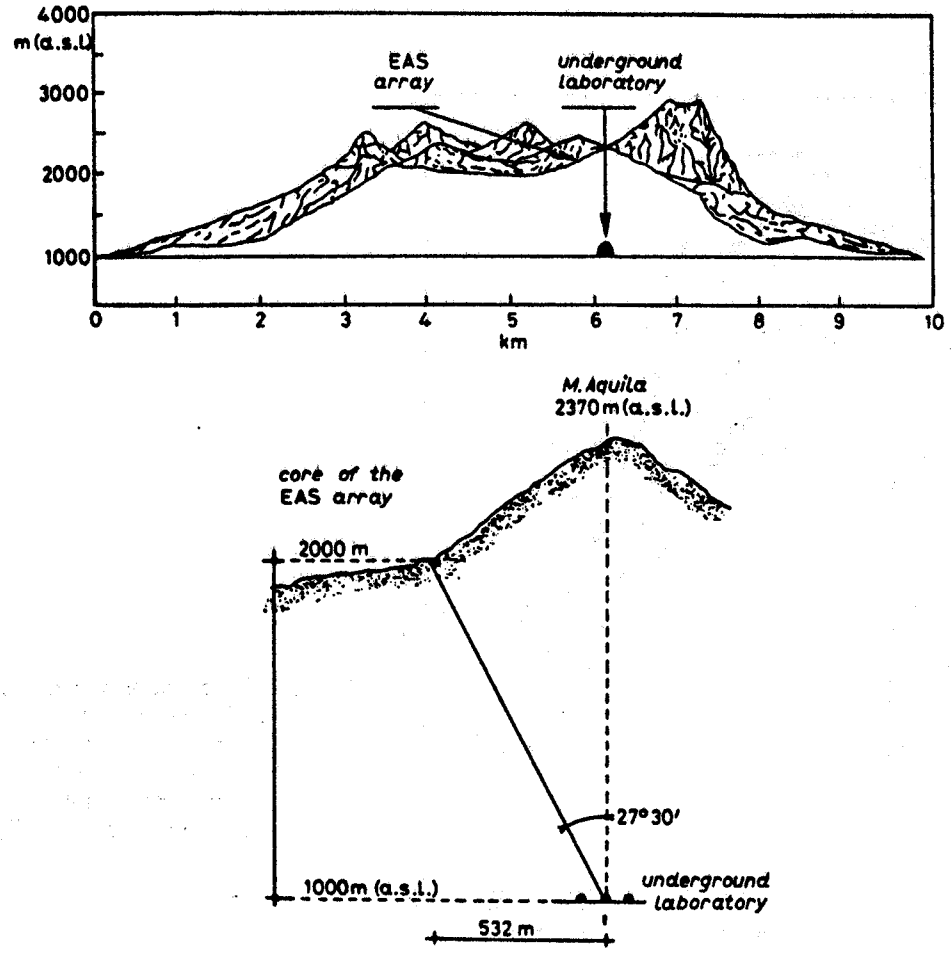

FIG. 4 - Profile of the mountain, location of the underground laboratory and of the EAS array.

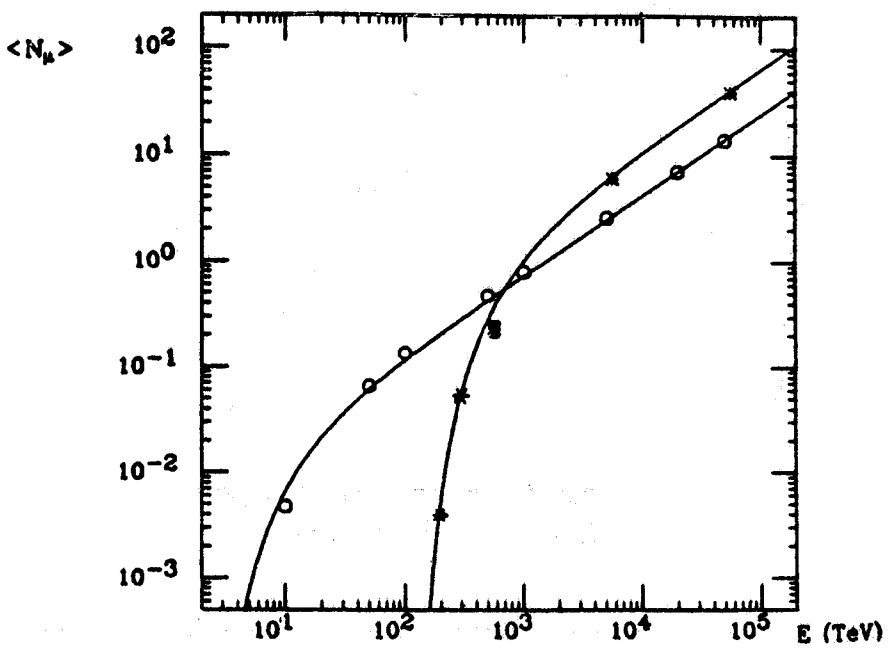

FIG. 5 - The mean number of muons from primary protons (open circle) and iron nuclei (stars) at depth of 4000 hg/cm^2 s.r. [Monte Carlo simulation, Ref.(13)]. Curves represent the parametrization given in Ref. (10) [Elbert's formula (1)].

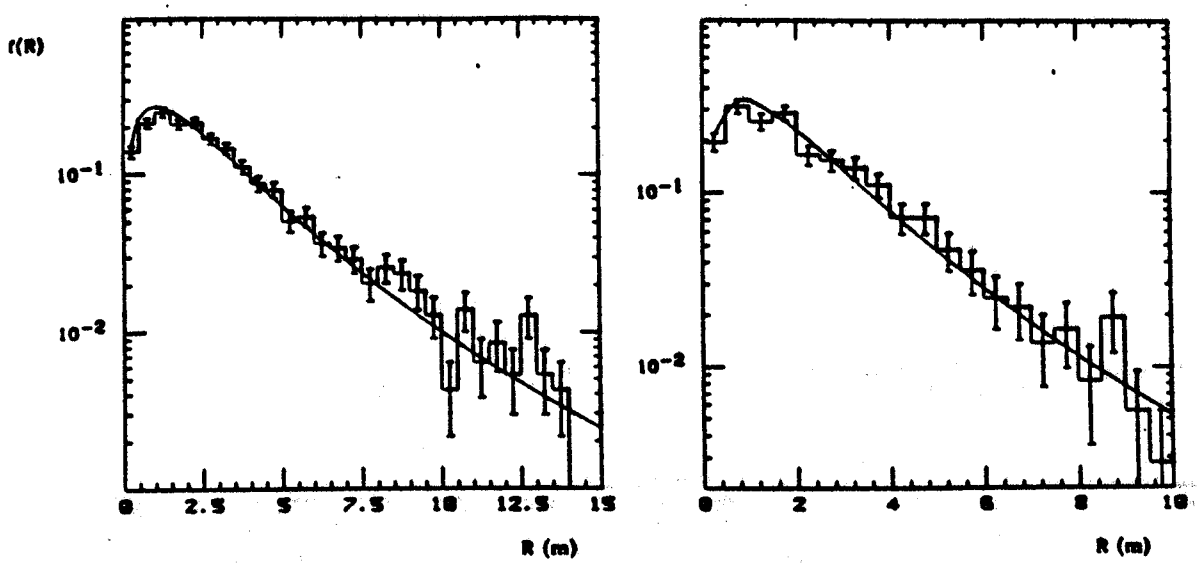

FIG. 6 - Muon lateral distribution f(R) = $1/N_\mu \cdot dN_\mu/dR$ at depths 3000 hg/cm^2 (left) and 4000 hg/cm^2 (right) from primary protons of energy 10^{15} eV.
Histogram: Monte Carlo simulation, Ref. (13);
Solid line : Parametrization used in calculating P_n (E_o, A).

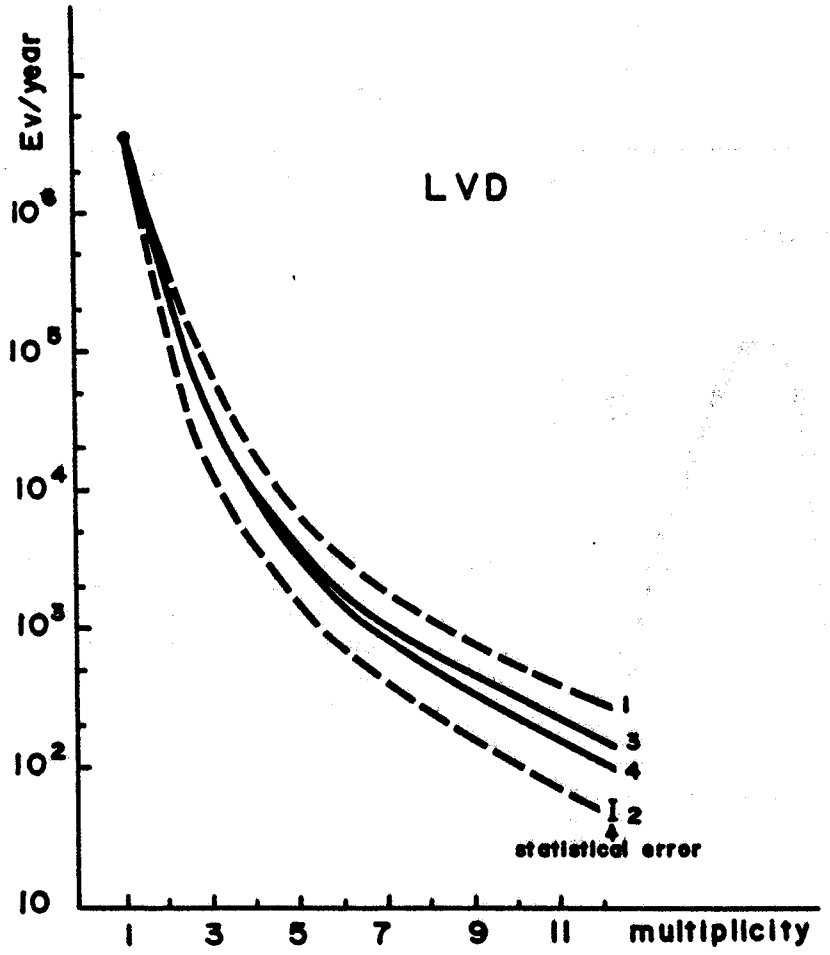

FIG. 7 -The calculated rates for multiple muons in LVD assuming the trial compositions "Maryland" (curve 1), LEC (curve 2), NUSEX with γ_{Fe} =2.6 (curve 3) or γ_{Fe}=2.7 (curve 4). The error bar indicates the statistical error on the flux of bundles of multiplicity 12 for one year of operation (LEC).

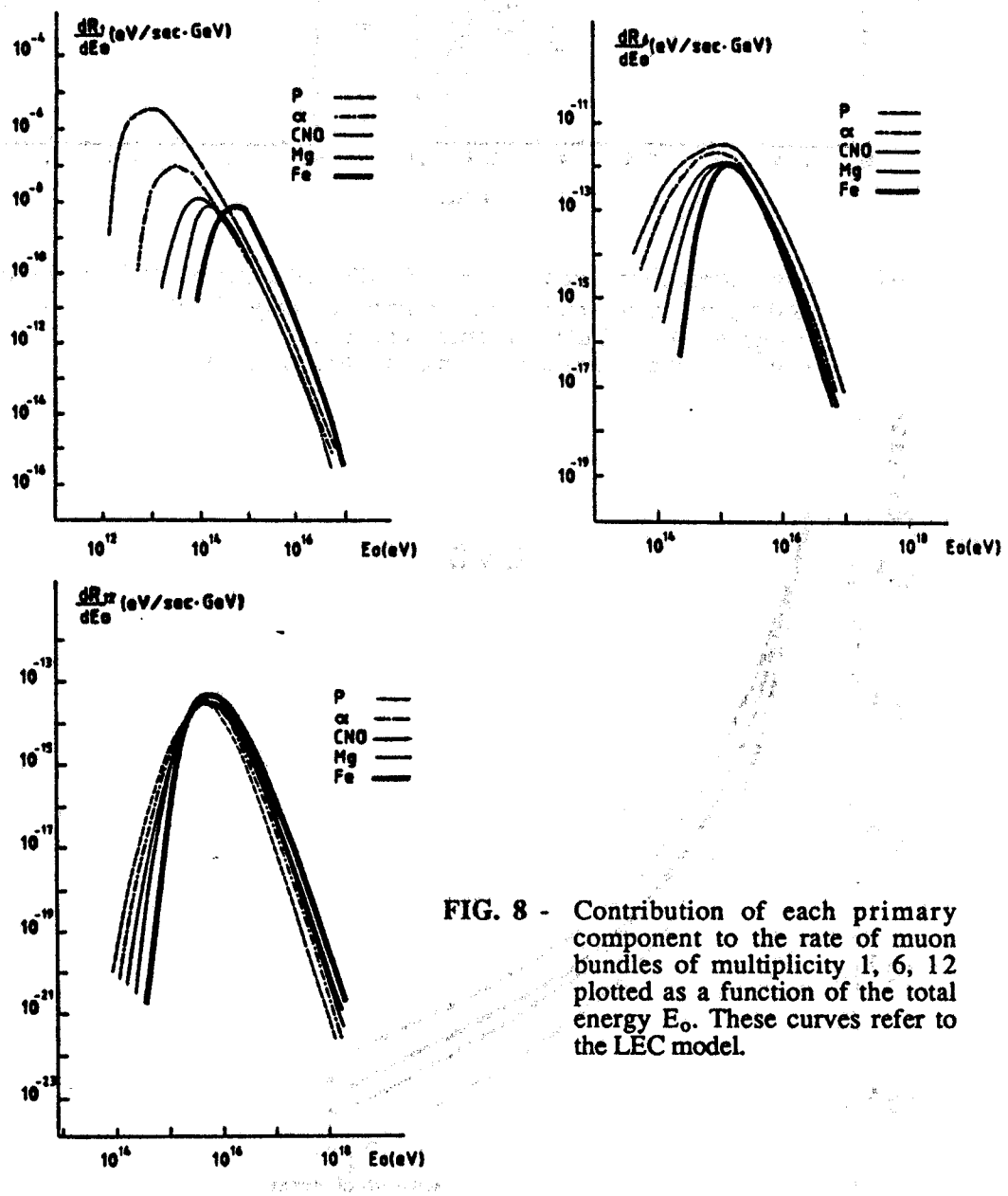

FIG. 8 - Contribution of each primary component to the rate of muon bundles of multiplicity 1, 6, 12 plotted as a function of the total energy E_o. These curves refer to the LEC model.

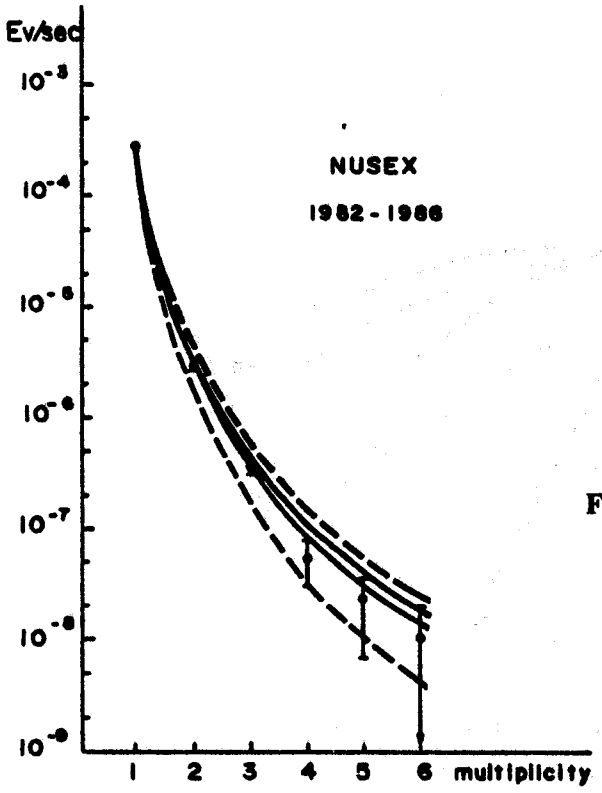

FIG. 9 - NUSEX data 1982 + 1986. Absolute comparison between the experimental rates of muon bundles and the predictions for the trial compositions "Maryland" (upper dashed line), LEC (lower dashed line), "NUSEX", $\gamma_{Fe} = 2.6$ (upper solid line) and $\gamma_{Fe} = 2.7$ (lower solid line).

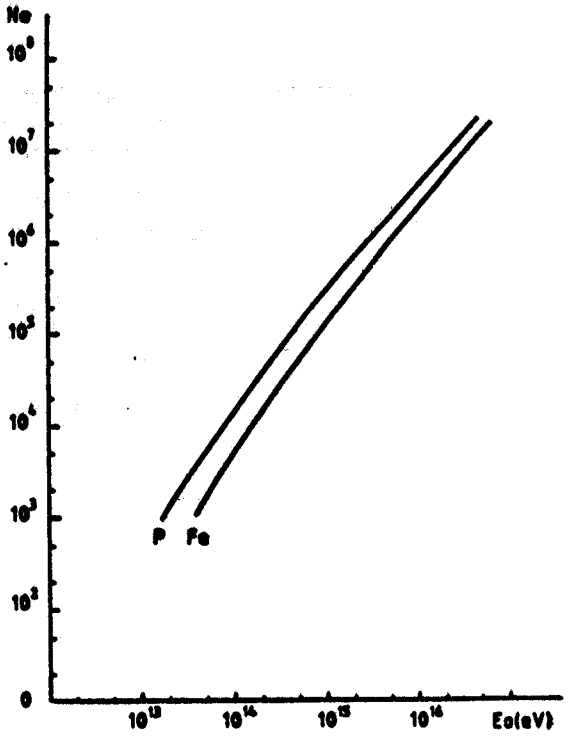

FIG. 10 - The relation between the size N_e at the G. Sasso altitude and the total energy E_o of primary cosmic rays (p = protons, Fe = iron nuclei). These curve refers to inclined showers ($\theta = 27.5°$).

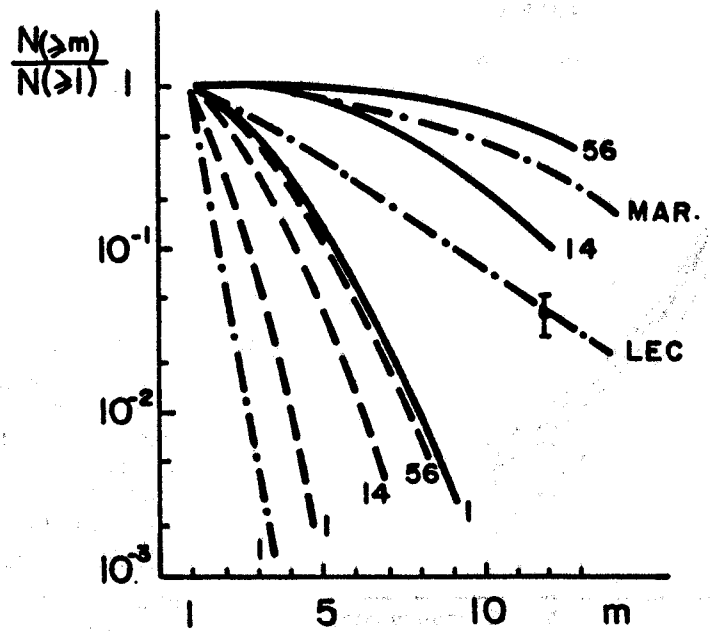

FIG. 11 - Muon multiplicity (m) integral distributions for intervals of the electron size N_e. The numbers identify the atomic mass of the primary (1: protons, 14: CNO group nuclei, 56: iron group nuclei).

Dash-dotted line: $10^4 < N_e < 3 \cdot 10^4$

Dashed lines : $10^5 < N_e < 3 \cdot 10^5$

Full lines : $10^6 < N_e < 3 \cdot 10^6$.

The expected muon multiplicity distributions for LEC and "Maryland" compositions have been calculated for events with shower size in the range $10^6 < N_e < 3 \cdot 10^6$ corresponding to primary energies above the knee.

The error bar indicates the statistical uncertainty on the normalized flux $N(\geq 12)/N(\geq 1)$ after two years of operation.

These results refer to an underground detector with an effective area of 500 m^2.

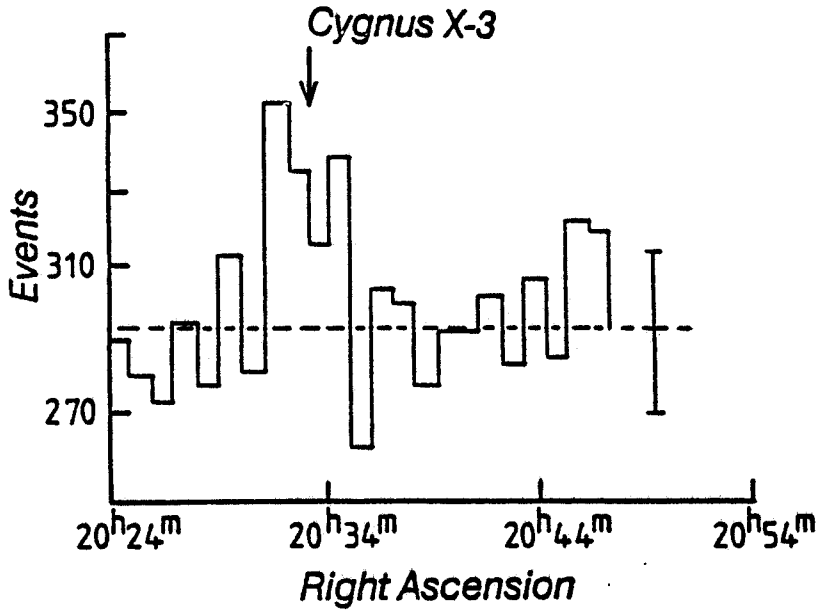

FIG. 12 - First observation of VHE γ-rays from Cygnus X-3 [Taken from Ref. (20a)].

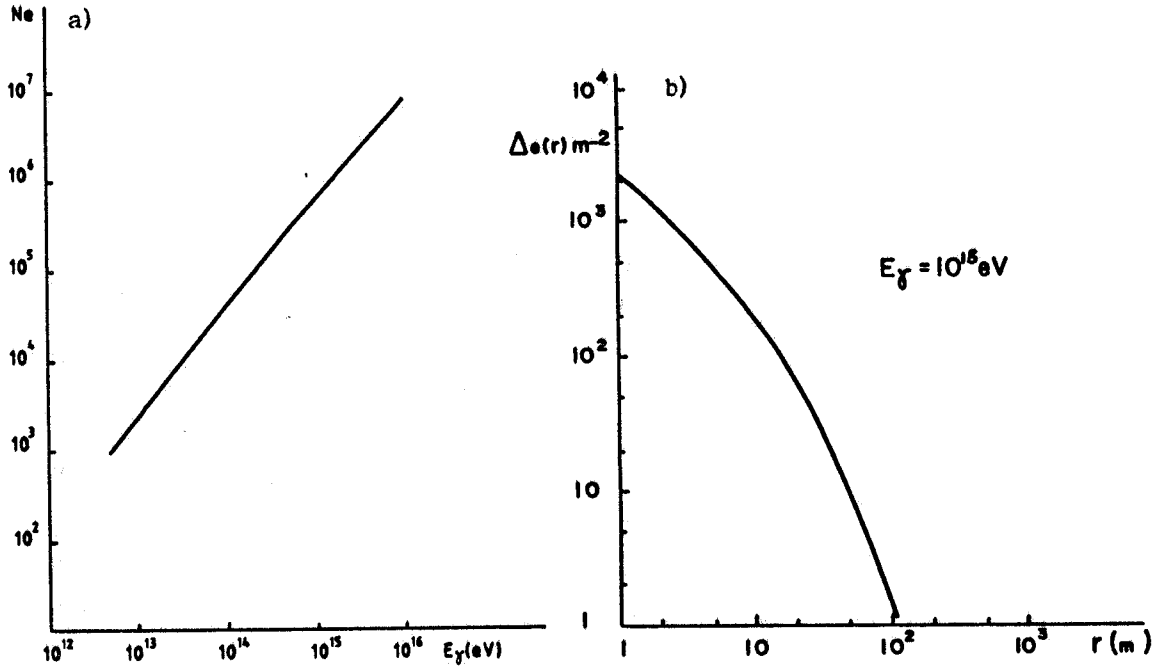

FIG. 13a - The electron size N_e at the G. Sasso (EAS-TOP) as a function of the primary γ-ray energy E_γ.

FIG. 13b - The electron density Δ_e as a function of the core distance for showers initiated by primary γ-rays of energy 10^{15} eV.

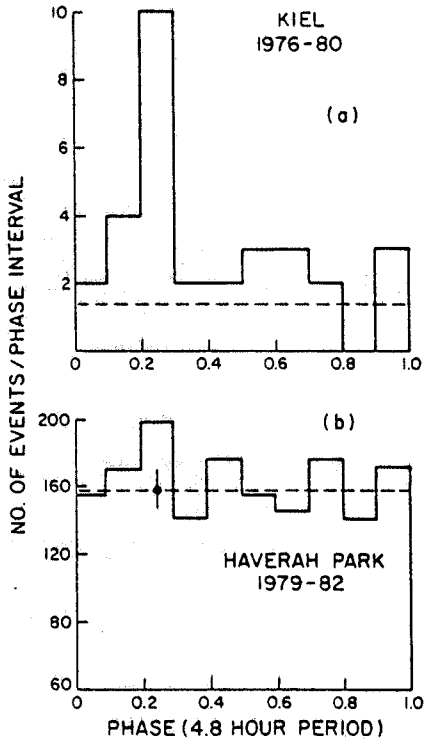

FIG. 14 - Light curves of the (a) Kiel and (b) Haverah Park data folded with the Mason ephemeris. [(Taken from T.C. Weeks, Ref. (17)].

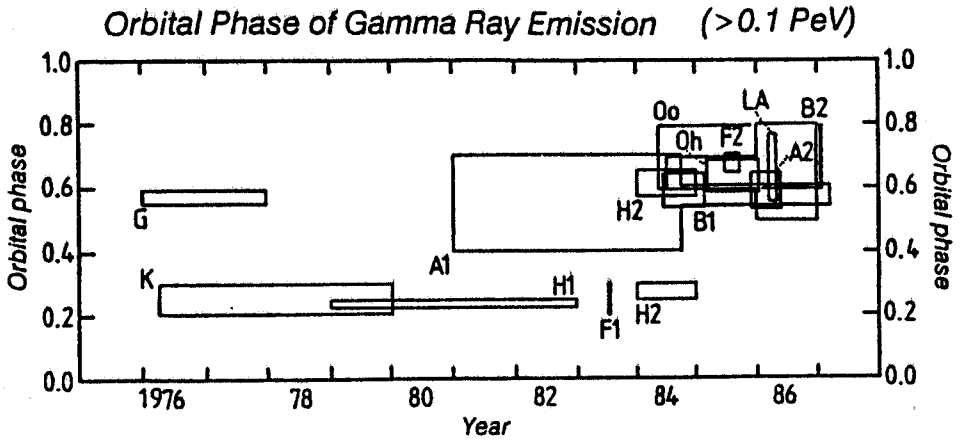

FIG. 15 - Orbital phase of γ-ray emission at energies above 10^{14} eV.
A1, A2 : Akeno; B1, B2 : Baksan; F1, F2 : Fly's Eye; G: Gulmarg; H1, H2 : Haverah Park; K : Kiel; LA : Los Alamos; Oh : Ohya; Oo : Ooty.
[Taken from Ref. (20a)].

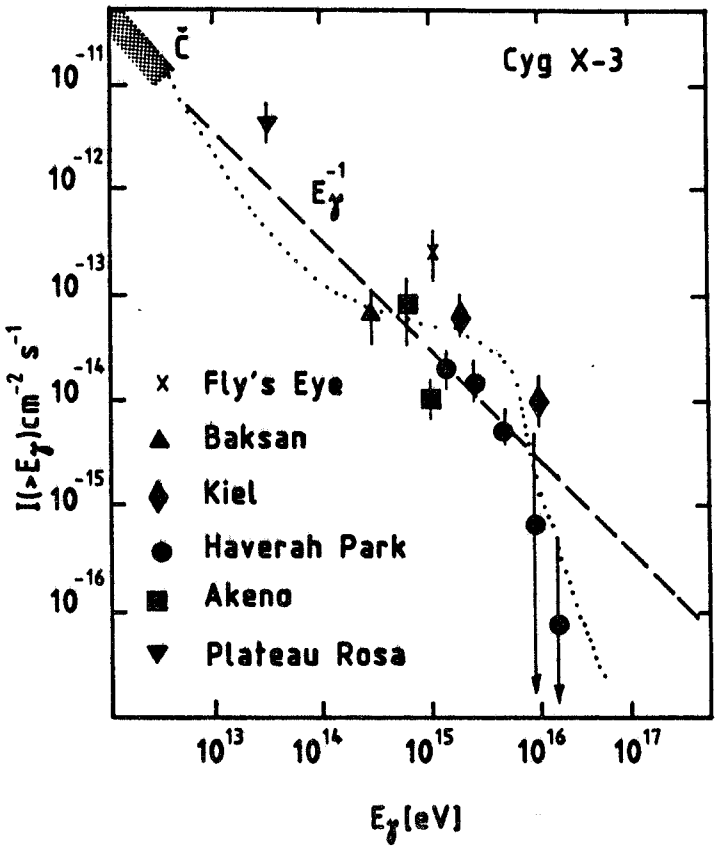

FIG. 16 - Time averaged energy spectrum of γ-ray observations from Cygnus X-3 (incomplete compilation). The dotted area corresponds to the detections by means of the air Cerenkov technique. The spectrum is very flat and can be fitted by a power law exponent of - 1. The dotted curve corresponds to the flux after correction to absorption of γ-rays on the microwave background radiation.

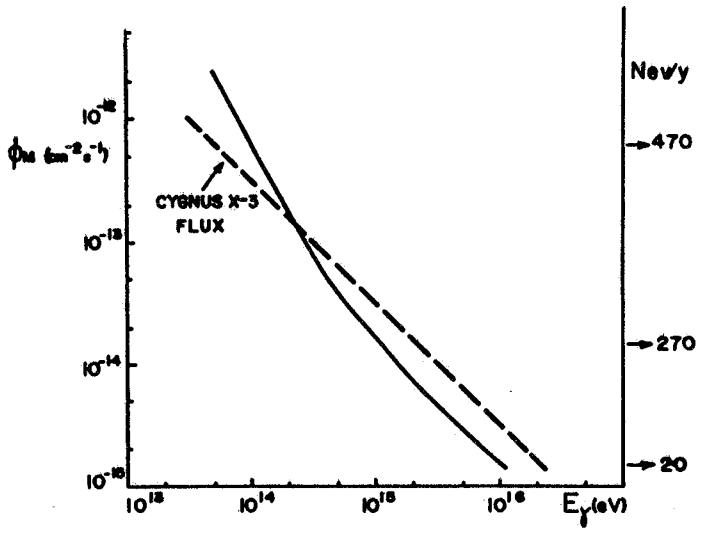

FIG. 17 - The minimum detectable flux from Cygnus X-3 at 3 σ before phase analysis for one year of EAS-TOP operation as a function of the γ-ray energy [observation time = 6 hours/day, angular acceptance = 2.5 · δθ]. Dashed curve corresponds to the experimental intensity. On the right side the number of events is shown.

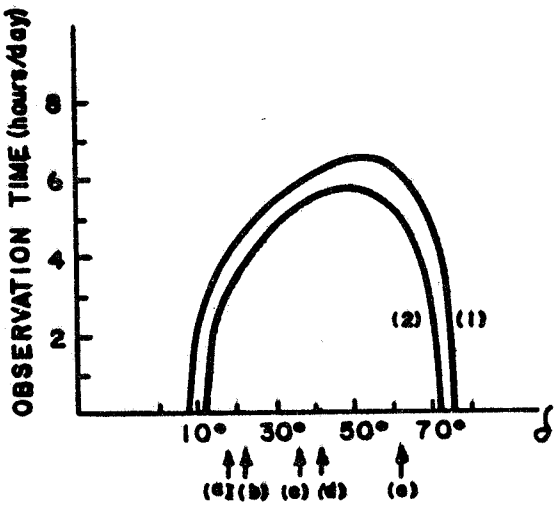

FIG. 18 - The observation time per day at EAS-TOP site as a function of the declination angle. Curve (1) is drawn assuming that the array is sensitive to air showers from within 35° of the zenith. Curve (2) has been calculated assuming an angular cut-off of 30°. Arrows indicate the declination of candidate sources:
(a) Geminga;
(b) Crab;
(c) Hercules X-1;
(d) Cygnus X-3;
(e) 4UO115 + 63.